

Direct experimental evidence of metastable epitaxial zinc-blende MgS

A. M. Sanchez,^{a)} J. Olvera, and T. Ben

Departamento de Ciencia de los Materiales e Ingeniería Metalúrgica y Química Inorgánica, Universidad de Cádiz, E-11510 Puerto Real (Cádiz), Spain

J. K. Morrod and K. A. Prior

School of Engineering and Physical Sciences, Brewster Building, Heriot-Watt University, Edinburgh, EH14 4AS, United Kingdom

S. I. Molina

Departamento de Ciencia de los Materiales e Ingeniería Metalúrgica y Química Inorgánica, Universidad de Cádiz, E-11510 Puerto Real (Cádiz), Spain

(Received 11 April 2006; accepted 21 July 2006; published online 18 September 2006)

High resolution transmission electron microscopy has provided direct experimental evidence of monocrystalline, single-phase zinc-blende MgS. The authors report the first high resolution images of a metastable β -MgS epilayer. This material naturally has rocksalt crystalline structure, but β -MgS was grown in this work by molecular beam epitaxy on a ZnSe/MgS multilayer buffered GaAs (001) substrate using Mg and ZnS sources, following a simple procedure. A metastable β -MgS layer of up to 125 nm thick has been examined using this technique. Embedded stacking faults are observed in the β -MgS thick epilayer. © 2006 American Institute of Physics.

[DOI: 10.1063/1.2353826]

Zinc-blende magnesium sulfide (β -MgS) is a wide band gap semiconductor material¹ ($E_g \sim 4.8$ eV) which has a number of unusual and useful physical properties. When used as a barrier material with most other II-VI semiconductors, it produces outstanding carrier confinement. For example, in the case of CdSe, the emission energy can be increased to over 3.7 eV.²

II-VI materials can adopt various crystalline structures, with both cubic and hexagonal symmetries. The stability of the crystal structure is related to the ionicity factor f_i and it also depends on the underlying substrate symmetry. The growth of II-VI semiconductors on (001) substrates generates cubic structures, which are metastable in materials having wurtzite crystalline structure in their stable phase. The Philips' ionicity of MgS is 0.786, close to the transition from wurtzite to the rocksalt structure.³ Nevertheless, it has been demonstrated that the free energy for the phase transformation between rocksalt and zinc blende is close to zero.⁴ As a result, in MgS, rocksalt is the naturally favored phase in epitaxial growth on GaAs(001), since the symmetry of the substrate surface cannot force the adoption of wurtzite phase and rocksalt structure presents the lowest energy crystal structure.

Despite this, the growth conditions have an enormous significance on the phase of the deposited epitaxial films. Therefore, it is possible to grow metastable β -MgS using certain growth conditions, although the growth of β -MgS is not straightforward since the crystal structure tends to transform into the most stable rocksalt.

Initial attempts to grow MgS by molecular beam epitaxy (MBE) and metal-organic chemical-vapor deposition succeeded in obtaining layers with a maximum thickness of 10 nm.^{5,6} However, recently a simple MBE growth procedure has been developed at Heriot-Watt University to in-

crease the layer thickness of this metastable β -MgS. Single layers of thickness over 60 nm are achievable, and layers over 130 nm have been routinely obtained using a MgS/ZnSe buffer layer to initiate growth.

Transmission electron microscopy (TEM) techniques provide structural information of most crystalline semiconductor materials.⁷⁻⁹ Nevertheless, while huge numbers of articles can be found in the literature about the structural characterization in III-V, III-N, and SiGe, fewer works on II-VI, and particularly on epitaxial MgS, have been produced. Additionally, no prior transmission electron microscopy images have been reported in the literature for epitaxial metastable β -MgS. In this work, we report the structural analysis and the first high resolution TEM (HRTEM) images of β -MgS.

Growth was performed in a Vacuum Generators V80H MBE system. In a similar manner to all previous Heriot-Watt MgS growths, deposition was made directly on a (100) GaAs substrate after *ex situ* etching and subsequent oxide removal in the MBE system, i.e., without the use of a GaAs buffer layer. Further growth details of the MgS growth can be found in Ref. 10. The analyzed heterostructure contains two β -MgS layers and was grown with the nominal structure ZnSe(5 nm)/MgS(134 nm)/ZnSe(10 nm)/MgS(25 nm)/ZnSe(5 nm)/GaAs(001). Thicknesses quoted are from growth rates obtained from calibration samples.

Cross section TEM specimens were prepared by mechanical grinding and dimpling down to 20 μ m, followed by ion milling to get electron transparency. In order to minimize the damage in the heterostructure, the specimen was milled successively decreasing the voltage from 6 to 1 kV. The specimen preparation is explained in more detail in Ref. 11. Conventional TEM, HRTEM, and selected area electron diffraction (SAED) were carried out on a Jeol 2011 and Jeol 2010 FEG transmission electron microscopes operating both of them at 200 kV. Observations were performed along the $\langle 110 \rangle$ GaAs for atomic characterization of the interfaces in the heterostructure.

^{a)} Author to whom correspondence should be addressed; FAX: +34 956 01 62 88; electronic mail: ana.fuentes@uca.es

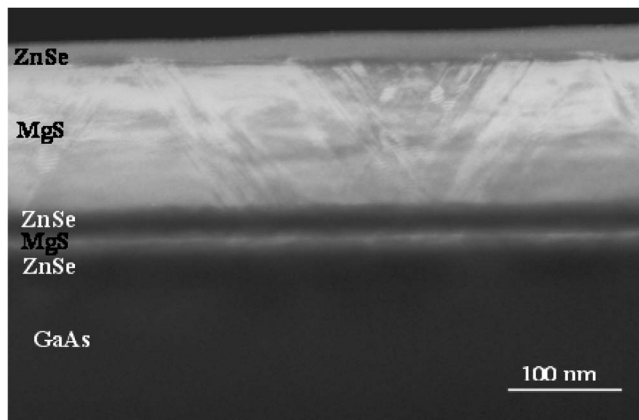


FIG. 1. Dark field cross-section TEM images recorded under two beam conditions for $g=002$ showing the different layers in the heterostructure.

Figure 1 shows a typical dark field 002 TEM image of the heterostructure. The MgS layers appear as bright regions between dark layers of ZnSe. An estimated thickness of 125 nm for the MgS thick layer can be obtained from this image. Stacking faults embedded in the metastable β -MgS thick layer are visible in the micrograph. These defects lie on the $\{111\}$ planes, with an angle of 54.73° with respect to the (001) interface plane. HRTEM was performed on MgS layers, with the orientation of the specimen along the $\langle 110 \rangle$ zone axis. The images were recorded around the Scherzer defocus. Figure 2 shows a HRTEM image of the MgS; the typical ABC stacking sequence for zinc-blende materials is present in the layer as can be observed in the micrograph. Additionally, HRTEM simulations were carried out along the $\langle 110 \rangle$ zone axis for defoci from 10 to 100 nm (underfocus) and thicknesses from 1 to 20 nm for both the rocksalt and zinc-blende MgS structures. Calculated images for thickness among 1 and 10 nm at Scherzer defocus are gathered in Fig. 3(a) for rocksalt and Fig. 3(b) for zinc-blende crystalline structures. These two different cubic structures possess a clear different appearance for the MgS. The rocksalt MgS presents a streaky pattern that was not observed experimentally in the analyzed heterostructure. SAED patterns recorded in areas containing only the MgS layer showed no extra spots; therefore if rocksalt phase or misorientated interfacial grains were embedded in the MgS layer, their size and/or quantity are not detectable using this technique. The analysis by HRTEM let

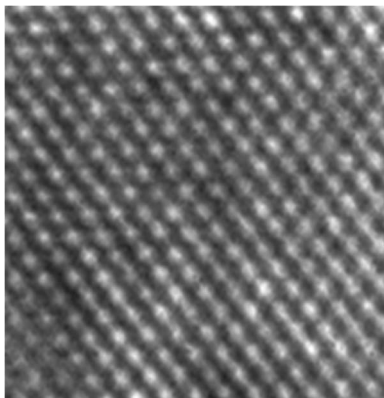


FIG. 2. HRTEM micrograph of MgS layer recorded around Scherzer defocus along the $\langle 110 \rangle$ zone axis.

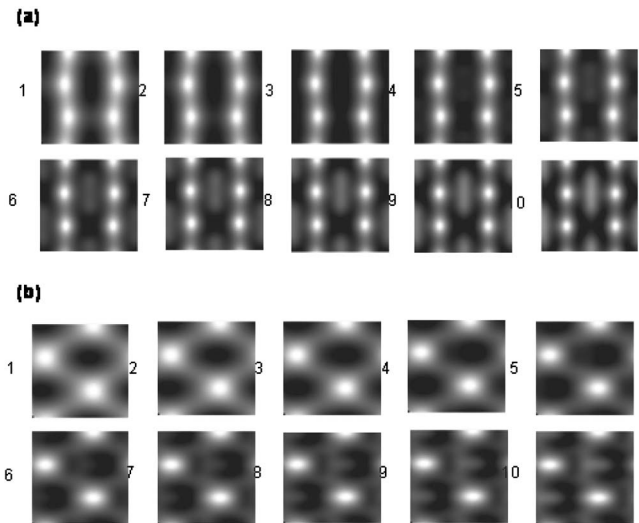


FIG. 3. Simulated HRTEM images in the thickness range of 1–10 nm at Scherzer defocus (a) rocksalt and (b) zinc-blende MgS.

us to conclude that the MgS is grown with metastable zinc-blende structure in this system.

Further HRTEM images were taken and analyzed in the different interfaces, as shown in Fig. 4. The HRTEM micrograph of Fig. 4(a) reveals a relatively rough interface of the first ZnSe epilayer with the GaAs substrate. This roughness could be explained by the surface preparation previously to the epitaxial growth and lead to the formation of a high density of stacking faults. The stacking faults have been observed in the whole heterostructure. This kind of defects lies in the four different $\{111\}$ planes constituting pyramidal planar defects, being confirmed by planar view TEM analysis (not shown in this letter).

A detailed analysis has been carried out of the ZnSe/MgS multilayer grown on the GaAs(001) before the thick β -MgS layer. TEM and HRTEM images showed a higher concentration of stacking faults in the MgS than in the ZnSe layer. The tensile interface MgS/ZnSe influences the generation of stacking faults and associated partial dislocations in the MgS,¹² increasing the defect concentration in the MgS layer with respect to the ZnSe. The MgS critical thickness was calculated using the geometrical theory proposed

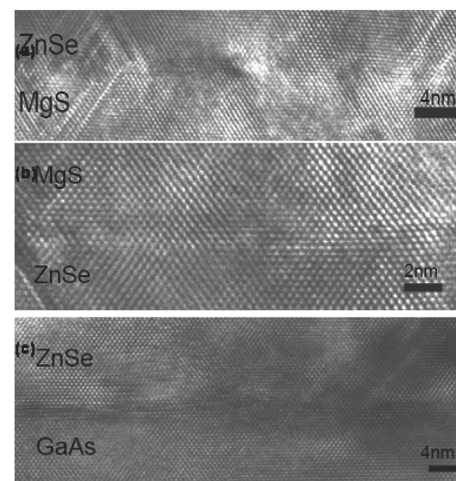


FIG. 4. $\langle 110 \rangle$ HRTEM micrographs of the different interfaces in the ZnSe/MgS multilayer (a) ZnSe/MgS, (b) MgS/ZnSe, and (c) ZnSe/GaAs(001).

by Dunstan *et al.*,¹³ and we found $h_c=22$ nm. This value is clearly below the estimated experimental one in the metastable thick β -MgS epilayer, ~ 125 nm, which is most likely completely relaxed.¹⁴

Summing up, direct experimental evidence of a metastable β -MgS epilayer has been reported. HRTEM images and SAED experiments have demonstrated single-phase zinc-blende MgS without the rocksalt phase. Therefore, metastable β -MgS thick layers can be achieved by means of the MBE growth procedure using Mg and ZnS sources. Stacking faults embedded in the MgS epilayers have also been observed.

This work was supported by the SANDiE Network of Excellence (Contract No. NMP4-CT-2004-500101) and the Junta de Andalucía (PAI research group TEP-0120). TEM measurements were carried out in the DME-SCCYT-UCA.

¹C. Bradford, C. B. O'Donnell, B. Urbaszek, A. Balocchi, C. Morhain, K.

- A. Prior, and B. C. Cavenett, *J. Cryst. Growth* **227/228**, 634 (2001).
²M. Funato, A. Balocchi, C. Bradford, K. A. Prior, and B. C. Cavenett, *Appl. Phys. Lett.* **80**, 443 (2002).
³J. C. Phillips, *Phys. Rev. Lett.* **27**, 1197 (1971).
⁴A. Navrotsky and J. C. Phillips, *Phys. Rev. B* **11**, 1583 (1975).
⁵N. Teraguchi, H. Mouri, Y. Tomomura, A. Suzuki, H. Taniguchi, J. Rorison, and G. Duggan, *Appl. Phys. Lett.* **67**, 2945 (1995).
⁶K. Uesugi, T. Obinata, H. Kumano, J. Nakahara, and I. Suemune, *Appl. Phys. Lett.* **68**, 844 (1996).
⁷A. Rosenauer, T. Remmele, D. Gerthsen, K. Tillmann, and A. Förster, *Optik (Stuttgart)* **105**, 99 (1997).
⁸S. Kret, P. Ruterana, A. Rosenauer, and D. Gerthsen, *Phys. Status Solidi B* **227**, 247 (2001).
⁹M. J. Hÿtch and T. Plamann, *Ultramicroscopy* **87**, 199 (2001).
¹⁰C. Bradford, C. B. O'Donnell, B. Urbaszek, A. Balocchi, C. Morhain, K. A. Prior, and B. C. Cavenett, *Appl. Phys. Lett.* **76**, 3929 (2000).
¹¹N. Wang and K. K. Fung, *Ultramicroscopy* **60**, 427 (1995).
¹²J. Petruzzello and M. R. Leys, *J. Appl. Phys.* **53**, 2414 (1988).
¹³D. J. Dunstan, S. Young, and R. H. Dixon, *J. Appl. Phys.* **70**, 3038 (1991).
¹⁴C. Bradford, C. B. O'Donnell, B. Urbaszek, K. A. Prior, and B. C. Cavenett, *Phys. Rev. B* **64**, 195309 (2001).